Opt electrical effects of Ag nanoparticles ink on Cerium Titanium ternary Films

ABSTRACT

Light sensing forms a basis of fabricating solar cells which in turn promise to avail clean and sustainable electrical suitable to make worthwhile contributions to solving global renewable-energy challenges. Current solar cell technology heavily relies on crystalline silicon wafers. Due to its challenges, great research interest is now directed towards thin-film solar cells. An attempt on organic semiconductors materials has presented much poorer charge transports and shorter exciton diffusion lengths than inorganic ones do. These have greatly limit the thickness of the photoactive layer in case of organic materials. Theoretically, materials with high electrical conductivity such as metal nanoparticles are opaque. They also offer lower optical transparency. Therefore, finding materials that are both transparent to visible light and electrically conductive is a continues study so that today's popular devices such as liquid-crystal displays and organic light-emitting diodes in televisions, touch screens in phones or tablet computers, electrophoretic displays in e-readers, or solar cells are visible. In this work, silver nanoparticles were used to dope cerium titanium dioxide by using a laser source at low pressure oxygen atmosphere irradiations. It was found that this procedure generated $Ce_xAg_{0.02x}TiO_2$ composite when pure cerium oxide, silver metal and titanium dioxide composites were used. The resulting thin films were found to possess higher absorption coefficients in the UV-visible spectral region accompanied with a tunable optical band gap varying between 3.42 eV to 3.78 eV. It was proposed to be suitable for wind band gap optical applications like in lasers design and applications.

Keywords: *$CeTiO_2$, Composite, $Ce_xAg_{0.02x}TiO_2$ thin films, laser radiation*

1. INTRODUCTION

Silver nanoparticles have proved to have various effective applications in technology. Dispersed Ag NPs on TiO_2 thin films alone was found to enhance the photocurrent generation with five folds as compared to TiO_2 under UV light irradiation [2]. Silver modifies many nano-composites under visible light irradiation for complete inhibition of microorganism activities. Cerium titanium dioxide trioxide has shown some useful functional properties promising technological applications especially in gas sensor technology and electrochromic devices [5].

By including metal nanoparticles silver or gold in a gas sensor [13], it is found to modify in their physical, chemical and structural properties. It has been found that gas sensor activity increase three times higher when loaded Ag nanoparticles under visible-light irradiation. It has also been found to effective enhance sensitivity and selectivity electrochromic devices [7]. They have also been proposed as effective in reducing the response [5] and recovery times in gas sensors [8, 15]. It is applications include removing biological impurities from drinking underground water supplies, modifying nanostructures through different processing methods like sol-gel procedures, magnetron sputtering [9], direct femtosecond laser irradiation or pulsed laser deposition [10]. In this study, pulsed laser deposition technique was used and we present results on the effect of silver nanoparticles $CeTiO_2$ thin films.

2. METHODOLOGY

2.1 Cleaning of Substrates

The SiO_2 quartz substrates were cleaned with acetone in a ultrasonic bath. The target was thoroughly cleaned before any preliminary trials were done and also after the trials.

2.2 Preparation of Vacuum Chamber

Prior to each irradiation the vacuum chamber was evacuated down to a residual pressure of 10^{-4} Pa. This pressure was maintained constant during the thin films synthesis process. High purity oxygen (99.9%) was then circulated inside the irradiation chamber through a calibrated gas inlet.

2.3 Reagents and Chemicals

The chemicals and reagents included cerium, titanium, silver, silicon substrate, high purity oxygen (99.9%) among other laboratory chemicals and apparatus.

2.4. Growth procedures

The growth of silver doped $CeTiO_2$ thin films was performed inside a stainless steel reaction chamber with a pulsed frequency laser fixed at λ = 255 nm, $\tau_{WHM} \sim 8$ ns, ν = 20 Hz; laser fluency fixed at 5 J/cm^2 at 0.1 MPa pressure. Silver nano-particle concentration was varied between 1.5 to 3 wt.% range and sintered at 1000 $^{\circ}$C for 2 hours. The substrates were positioned at a separation distance 30 mm from the target surface and parallel to it. The substrate temperature was fixed at about 630 ^{0}C during the film growth and only 10,000 laser

pulses were applied to each thin film. The films were cooled down with a ramp of about 10 ^{0}C per minute at 0.5 MPa that used during the deposition experiments.

2.5 Thin film characterization

The optical measurements were performed with a double beam Perkin Elmer Lambda 19 spectrophotometer in the wavelength range of 300nm to 1100 nm while compositional and crystallinity status were investigated by XRD and EXRD measurements by configuring the X-ray diffraction in θ-2θ configuration with a Philips MRD diffractometer (CuKα, λ=1.5418 Å radiation).

3.0 RESULTS

3.1 Elemental Composition of $CeTiO_2$

The obtained SAED pattern resulted into inter-planar distances of 0.385 and 0.192 nm assigned to the (001) and (002) lattice plane reflections of the orthorhombic $CeTiO_2$ phase [4,7], with lattice parameters a = 7.318 Å, b = 7.451 Å, and c = 3.684 Å, as referred in the JC-PDS 20-1324. Hence, there was no indication of the presence of silver or silver oxide observed.

3.2 Structural Properties of $CeTiO_2$ Thin films

The crystalline structure of the thin films was investigated using the XRD technology. The observed diffractogram curves composed of diffraction lines at 23.1°, 47.2° and 50.4° attributed to the (001), (002) and (112) lattice plane reflections. This implied an orthorhombic phase with a preferred orientation along the [001] crystal direction. With increase in Ag concentration, the intensity of the 23.1° line corresponding to (001) lattice plane reflection decreased gradually with full width at half maximum increasing [9].

3.2.1 Structural Properties silver doped of $CeTiO_2$ Thin films

Adding silver nano-particles to the film, the XRD peaks were modified. It was attributed the line 23.6° that appeared at (020) lattice plane reflection. About 0.2° degree shift towards higher values on the line was observed that corresponded to (001) lattice plane reflection. This was also attributed to the slight change of the d-spacing lattice parallel to the surface of substrate. It was concluded that silver nanoparticles as a dopant lead to an increase in the average dimensions crystals. The average size of nanocrystallites in the films was determined by the Scherrer equation [10]:

$$D_{hkl} = \frac{0.9\lambda}{\beta_{hkl} \cos\theta_{hkl}} \quad (1.1)$$

where λ is the X-ray wavelength, θ_{hkl} is the Bragg diffraction angle and β_{hkl} is the full width at half-maximum.

3.3. Optical properties

3.3.1 Chromaticity coordinates and tristimulus

It is known that chromaticity coordinates are used to specify the colour observed according to the CIE chromaticity diagram. Equally, standard tristimulus value is used as a measure of the brightness of a surface or colour. By using Pyton 2.7 program [1, 2, 9], optical transmittance spectra, chromaticity coordinates and standard tristimulus value were calculated and tabulated as shown in table I and it is graphically represented by figure 1. The dark blue colour was attributed to oxygen deficiency in the thin films. This further implied that $CeTiO_2$ underwent partial decomposition at the target as it was being irradiated by the subsequent laser pulses.

Table I: ***Chromaticity coordinates and tristimulus of doped thin films***

Ag conc. wt.%]	***Chromaticity coordinates*** **(x, y)**	***Tristimulus*** **Y**	**Colour Status**
3.0	(0.35, 0.34)	817	Dark blue
2.5	(0.29, 0.32)	321	slightly Transparent
2.0	(0.23, 0.16)	19	Fairly transparent
1.5	(0.18, 0.16)	9	Transparent
1.0	(0.14, 0.13)	3	Very transparent
0.5	(0.12, 0.11)	1	Very transparent
0.0	(0.11, 0.1)	1	Very transparent

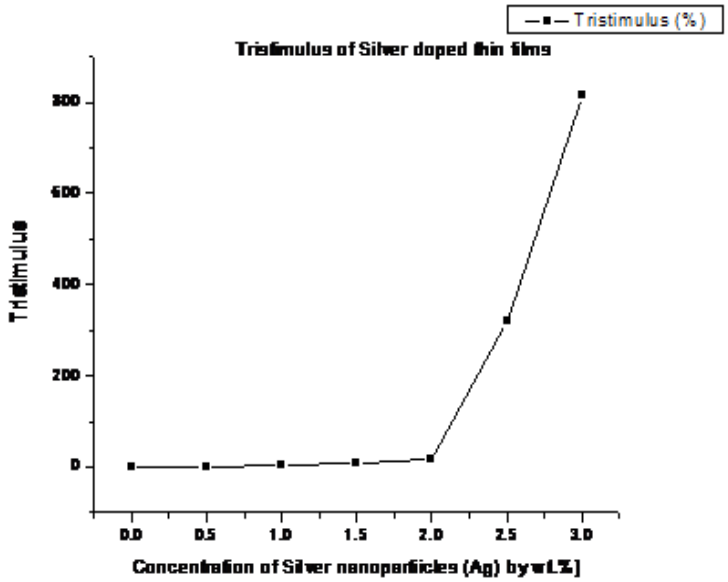

Figure 1: ***Tristimulus of doped thin films***

3.3.2 Optical Transmittance

The average transmittance of the un-doped $CeTiO_2$ film was close to 90 % in the visible spectral range while the one containing silver (Ag) had an average decrease of greater than 20 %. This was attributed to the formation of oxygen vacancies at low supply oxygen [3] since this low supply pressure does not stabilize stroichiometric formation of $CeTiO_2$ crystals.

3.3.3 Optical Absorption

Optical absorption increased as Ag concentration increased. This was attributed to the surface plasmon resonance absorption resulting from the embedded Ag nano-particles as the absorption was observed to shift towards higher wavelengths as silver concentration increased. SPR peak positions below 410 nm were observed at very low Ag nano-particle concentrations and thus optical absorption coefficient, α, was calculated from [4];

$$\alpha = A \ln \frac{10}{d} \qquad (1.2)$$

where ***A*** stands for the absorbance and ***d*** for the thickness of the films.

3.3.4 Determination of thickness

Using surface profilometry data, the average thickness of the un-doped and doped thin films was evaluated to be around 98 nm.

3.3.5 Optical Band Gap, E_g

Fundamentally absorption coefficient follows the relation in Eq. 4 where m = 2 for the indirect transitions and ½ for directly allowed transitions [9];

$$\alpha h\nu \sim (h\nu - E_g)^m \quad (3)$$

The Scout Software was used determine the possible transitions by simulating $(\alpha h\nu)^{1/m}$ against $h\nu$, photon energy for m = 2 and for m = ½. Table II shows the obtained band gaps.

Table II: Band gaps for Thin films

$CeTiO_2$	$Ce_xAg_{0.02x}TiO_2$
2.66	3.42
2.78	3.55
2.87	3.76
3.03	3.79

This was similar to determining the band gap from plots of Eq. 4 for direct band gap values can be estimated [10];

$$(\alpha h\nu)^2 \sim h\nu - E_g \quad (4)$$

Band structure calculations were done on $CeTiO_2$ thin films (*reported elsewhere*- Mosiori *et al., 2*016) revealed oxygen deficiency. The narrow changes observed in band gaps was attributed to charge carrier transfer from Ag to $CeTiO_2$ layer that might have resulted into a downward shift of the conduction band and at the same time, an upward shift of the valence band hence increasing the band gap, E_g.

3.3.6 Urbach energy, E_0

As observed in Mosiori *et al.* 2016, at photon energy *hv*, below the absorption edge, it is possible to evaluate the Urbach energy or the Urbach tail. This is because the structural disorders observed generate band tails with localised states and therefore the Urbach energy, $\mathbf{E_0}$, can easily be estimated from [5];

$$\alpha(h\nu) = \alpha_o e^{(\frac{h\nu}{E_o})} \quad (1.3)$$

This means that the dependence of Urbach energy on Ag concentration may introduce some lattice disorder in the composite material.

Table III: A***verage size and Urbach Energy***

Ag concentration [wt.%]	Nano-crystallites size [nm]	Urbach energy [meV]

3.0	85	297
2.5	63	361
2.0	51	398
1.5	41	421
1.0	33	441
0.5	29	496
0.0	17	573

If this expression is used to plot a curve, then the inverse of the slope will be a linear fit to the logarithmic plot of the absorption coefficient [7]. The value of Urbach energy calculated in this work as shown in table III and further illustrated by figure 2 was fairly similar for undoped $CeTiO_2$ thin films as reported in literature elsewhere by other growth methods [3, 6, 8,11].

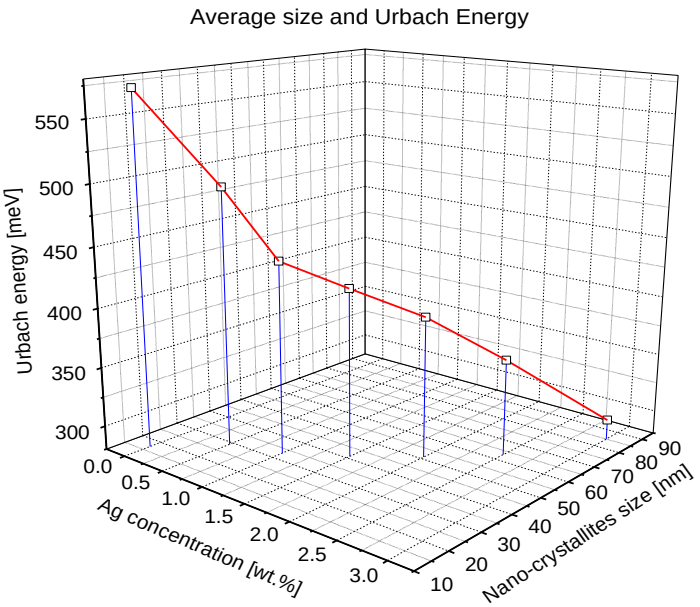

Figure 2: Relationship between average Silver particle and Urbach energy

3.4 Electrical properties

3.4.1 Current-Voltage curve by CSAFM on $CeTiO_2$ thin films

CSAFM technique was used to determine the local conductivity of $CeTiO_2$ thin films using biased Pt-Ir coated silicon tips in contact mode. All the curves were non-ohmic as depicted by table IV. It was observed that the turn-on voltage value ranged between 0.1V to 0.3V while

their corresponding resistance at 0 V range from about 0.4 GΩ to 2.5 GΩ. The small element of conduction was attributed to the semiconducting properties [12] of $CeTiO_2$ thin films.

3.4.1 Current-Voltage curve by CSAFM on Ag doped $CeTiO_2$ thin films

Almost similar I-V curves were obtained for Ag doped $CeTiO_2$ thin films but the curves were slightly or nearly-ohmic in character. The slight deviation from the linearity was attributed to the contribution of the semiconducting behaviour [11] of $CeTiO_2$ while the ohmic behaviour was sttributed to the presence of evenly dispersion Ag nanoparticles present. From table IV and as depicted in figure 2, the gradual transition behaviour of I-V curve is a property that can be used in sensor applications to ensure better selectivity and sensitivity.

Table IV- Current-Voltage curve by CSAFM technique.

Thin Film	**CSAFM** Measurements											
	Voltage (μV)	-0.5	-0.4	-0.3	-0.2	-0.1	00	0.1	0.2	0.3	0.4	0.5
$CeTiO_2$	Current (*n*A)	-6	-4	-2	-1.5	-0.1	0.0	0.1	1.1	2.1	3.9	7.3
$CeAgTiO_2$	Current (*n*A)	-	-	-6.1	-4	-1	0.0	1.9	3.9	7.1	-	-

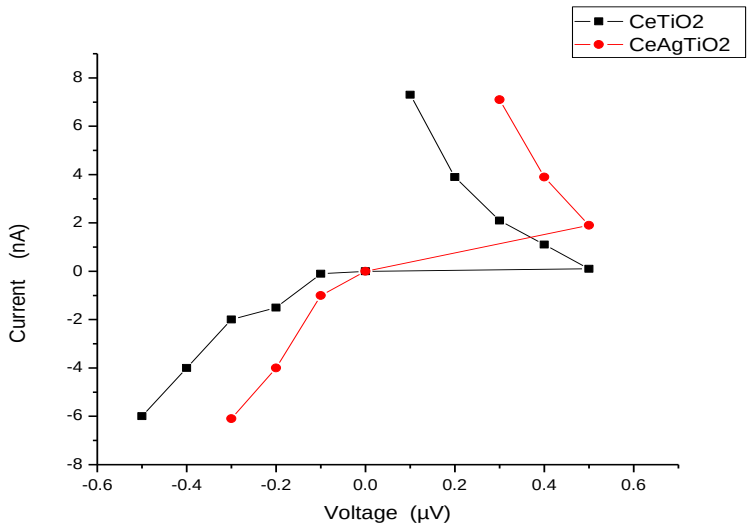

Figure 4: Comparison of I-V curve by CSAFM technique for $CeTiO_2$ aand $CeAgTiO_2$.

Conclusions

A nano-composite films of $Ce_xAg_{0.02x}TiO_2$ were grown by pulsed laser deposition. The effect of Ag concentration on crystalline status and optical properties was investigated. It was observed that there was a gradual band gap increase. This was attributed to the thin film's change in chemical composition as Ag was introduced. Electrical properties portrayed promising features for the design of new composite materials for applications electrochromic devices and gas sensors.

References

1. Ritala, M., Leskelä, M., Nykänen, E., Soininen, P., & Niinistö, L. (1993). Growth of titanium dioxide thin films by atomic layer epitaxy. *Thin Solid Films*, *225*(1), 288-295.

2. Arabatzis, I. M., Stergiopoulos, T., Bernard, M. C., Labou, D., Neophytides, S. G., & Falaras, P. (2003). Silver-modified titanium dioxide thin films for efficient photodegradation of methyl orange. *Applied Catalysis B: Environmental*, *42*(2), 187-201.

3. Machida, M., Norimoto, K., & Kimura, T. (2005). Antibacterial activity of photocatalytic titanium dioxide thin films with photodeposited silver on the surface of sanitary ware. *Journal of the American Ceramic society*, *88*(1), 95-100.

4. Hass, G. (1952). Preparation, properties and optical applications of thin films of titanium dioxide. *Vacuum*, *2*(4), 331-345.

5. Justicia, I., Ordejón, P., Canto, G., Mozos, J. L., Fraxedas, J., Battiston, G. A., ... & Figueras, A. (2002). Designed Self-Doped Titanium Oxide Thin Films for Efficient Visible-Light Photocatalysis. *Advanced Materials*, *14*(19), 1399-1402.

6. Argall, F. (1968). Switching phenomena in titanium oxide thin films. *Solid-State Electronics*, *11*(5), 535-541.

7. Sberveglieri, G., Comini, E., Faglia, G., Atashbar, M. Z., & Wlodarski, W. (2000). Titanium dioxide thin films prepared for alcohol microsensor applications. *Sensors and Actuators B: Chemical*, *66*(1), 139-141.

8. Suzuki, T., Kosacki, I., Anderson, H. U., & Colomban, P. (2001). Electrical conductivity and lattice defects in nanocrystalline cerium oxide thin films. *Journal of the American Ceramic Society*, *84*(9), 2007-2014.

9. Keomany, D., Poinsignon, C., & Deroo, D. (1994). Sol gel preparation of mixed cerium—titanium oxide thin films. *Solar Energy Materials and Solar Cells*, *33*(4), 429-441.

10. Younis, A., Chu, D., & Li, S. (2012). Oxygen level: the dominant of resistive switching characteristics in cerium oxide thin films. *Journal of Physics D: Applied Physics*, *45*(35), 355101.

11. Yoshimoto, M., Shimozono, K., Maeda, T., Ohnishi, T., Kumagai, M., Chikyow, T., ... & Koinuma, H. (1995). Room-temperature epitaxial growth of CeO2 thin films on Si (111) substrates for fabrication of sharp oxide/silicon interface. *Japanese Journal of Applied Physics*, *34*(6A), L688.

12. Bhuiyan, M. S., Paranthaman, M., & Salama, K. (2006). Solution-derived textured oxide thin films—a review. *Superconductor Science and Technology*, *19*(2), R1.

13. Keomany, D., Poinsignon, C., & Deroo, D. (1994). Sol gel preparation of mixed cerium—titanium oxide thin films. *Solar Energy Materials and Solar Cells*, *33*(4), 429-441.